Research Paper
Computational Methods for Differential Equations
http://cmde.tabrizu.ac.ir
Vol. *, No. *, *, pp. 1-17
DOI:10.22034/cmde.2026.70410.3499

Robust hybrid difference scheme for singularly perturbed reaction-diffusion equations with discontinuous source terms

Kousalya Ramanujam* **and Vembu Shanthi**

Department of Mathematics, National Institute of Technology, Tiruchirappalli - 620015, Tamil Nadu, India.

Abstract

This paper examines a system of two singularly perturbed reaction-diffusion type problems with Robin boundary conditions and discontinuous source terms. The equations are weakly coupled, leading to solutions that exhibit interior and boundary layers. To resolve these layers, a hybrid numerical scheme combining the cubic spline approximation technique and the central difference scheme is applied on a piecewise-uniform mesh of Shishkin type. This approach achieves nearly second-order convergence. The cubic spline approximation is applied in the boundary layer region. A central difference scheme with an average approximation of the source term is applied at the discontinuity point, whereas standard central difference technique is used elsewhere. The effectiveness of the proposed method is demonstrated through several test problems, and its performance is compared with that of a standard finite difference scheme.

Keywords. Singularly perturbed, Hybrid scheme, Robin boundary conditions, Shishkin mesh, Interior layer.
2010 Mathematics Subject Classification. 65H10, 65L11, 65L70.

Uncorrected

1. Introduction

The modeling of semiconductor devices often results in singular perturbation problems due to the vastly different scales of the underlying physical processes. Sharp variations in quantities, such as carrier concentrations and electric potentials near interfaces, lead to boundary and interior layers. Markowich [21] investigated the mathematical modeling of a semiconductor device under an applied bias in one-dimensional case. The model is governed by a set of ordinary differential equations, with boundary conditions applied at the contact points. Also, in [20] the author examines a system of singularly perturbed Robin problems derived from fundamental semiconductor equations, demonstrating the occurrence of boundary as well as interior layers.

The modeling of interaction between turbulence in water waves and currents is a complex problem. To account for turbulence effects in hydraulics, the standard $k-\varepsilon$ model is used by Rodi [28]. Using this model, Thomas et. al [34] derived a hierarchial system of equations to describe wave-current interactions. Each system consists of two second-order boundary value problems that are singularly perturbed, with experimental data indicating the formation of two interacting layers in the solutions. For more recent applications of singular perturbation theory, see [17, 18, 33, 35].

Recent studies including [13, 14, 16, 30] highlight the ongoing research interest in singularly perturbed Robin-type problems. A system of weakly coupled reaction-diffusion equations with linear coefficients and Dirichlet boundary conditions is studied by Matthews et al. [22, 23] and Madden et al. [19], each addressing a different case depending on the relationship between the singular perturbation parameters. Natesan [26] developed a hybrid scheme using central difference scheme and cubic spline techniques for the case, where one of the parameters is equal to one. Babu et al. [3] used the finite element method to solve the same Dirichlet problem with a discontinuous source term for a system with equal perturbation parameters. Rao [27] considered the problem with different parameters. Das et al. [8] proposed

Received: 26 November 2025; Accepted: 15 November 2026.
* Corresponding author. Email: ramanujamkousalya@gmail.com.

a hybrid scheme for the problem with Robin boundary conditions (1.3), achieving nearly second-order convergence regardless of the perturbation parameter.

Ansari [2] studied a convection-diffusion type Robin problem in the one-dimensional case, showing an order of convergence almost one. Basha et al. [5] solved (1.1) with Robin boundary conditions (1.3) and a point of discontinuity in the source term (1.2), assuming equal perturbation parameters. Chawla et al. [6] addressed a more general case of the problem with non-smooth data, applying the cubic spline technique at the boundaries.

From the above literature, it is evident that the central difference scheme together with Dirichlet boundary conditions achieves almost second-order convergence of order $\mathcal{O}(N^{-2}\ln^2 N)$ on a Shishkin mesh (cf. [22, 23]). However, for Robin-type boundary conditions of the form (1.3), the presence of first derivative terms reduces the accuracy of standard forward and backward difference schemes to almost first-order convergence, namely $\mathcal{O}(N^{-1}\ln N)$. To overcome this drawback, spline-based approximations for the Robin boundary conditions were introduced in [8], improving the convergence order to $\mathcal{O}(N^{-2}\ln^2 N)$.

In the present work, problems containing interior layers are also considered, and a central difference scheme is employed at the point of discontinuity to preserve the same order of convergence. Furthermore, cubic spline approximations are incorporated within the boundary layer regions to further enhance the convergence rate to $\mathcal{O}(N^{-2}\ln^2 N + N^{-\sigma_0\sqrt{\lambda}})$. Hence, among the methods available in the literature, the proposed method attains the best known order of convergence on the Shishkin mesh, which remains one of the most widely used fitted meshes for singularly perturbed problems. Motivated by the works of Basha et al. [5] and Chawla et al. [6], the present study extends the work of Das [8] to problems with nonsmooth data (cf. [7, 15, 31, 32, 36, 37]).

This paper examines a linearized problem that neglects the coupling between the highest derivative terms. The presence of Robin boundary conditions causes the solution to develop boundary layers. Additionally, a discontinuous source term gives rise to interior layers. To handle these features, a cubic spline technique as given in [1] is applied in the boundary layer region, while standard central differencing is used in the other regions, including the point of discontinuity. Let $D := (0,1)$ and let $\eta \in D$ be a point of jump discontinuity. Define the subdomains as $D^- := (0,\eta)$ and $D^+ := (\eta,1)$. The jump of a function y at η is expressed as $[y](\eta) = y(\eta^+) - y(\eta^-)$. Now, consider the following boundary value problem involving a system of weakly coupled reaction-diffusion equations with linear terms, defined on the unit interval D, with a non-smooth source term.

$$\mathbf{P}\vec{y} := \begin{pmatrix} -\varepsilon\dfrac{d^2}{dt^2} & 0 \\ 0 & -\varepsilon\dfrac{d^2}{dt^2} \end{pmatrix}\vec{y} + B\vec{y} = \vec{f} \quad \text{for } t \in D^- \cup D^+, \tag{1.1}$$

and B is a 2×2 matrix whose (i,j) entry is b_{ij} for $1 \leqslant i,j \leqslant 2$, given by

$$B = \begin{pmatrix} b_{11} & b_{12} \\ b_{21} & b_{22} \end{pmatrix}.$$

The discontinuous source term is defined as $\vec{f}(t) = \big(f_1(t), f_2(t)\big)^T$, where

$$f_1(t) = \begin{cases} f_{11}(t), & t \in [0,\eta], \\ f_{12}(t), & t \in (\eta,1], \end{cases} \quad \text{and} \quad f_2(t) = \begin{cases} f_{21}(t), & t \in [0,\eta], \\ f_{22}(t), & t \in (\eta,1]. \end{cases} \tag{1.2}$$

The operator $\mathbf{P}$ is $\mathbf{P}\vec{y} = (P_1\vec{y},\ P_2\vec{y})^T$, where

$$P_1\vec{y} \equiv -\varepsilon y_1'' + b_{11}y_1 + b_{12}y_2 = f_1,$$
$$P_2\vec{y} \equiv -\varepsilon y_2'' + b_{21}y_1 + b_{22}y_2 = f_2.$$

The Robin boundary conditions at ∂D are given by

$$\begin{cases} \mathcal{R}_1^{(0)}\vec{y}(0) \equiv \alpha_1 y_1(0) - \sqrt{\varepsilon}\beta_1 y_1'(0) = p_1, & \mathcal{R}_1^{(1)}\vec{y}(1) \equiv \gamma_1 y_1(1) + \sqrt{\varepsilon}\delta_1 y_1'(1) = q_1, \\ \mathcal{R}_2^{(0)}\vec{y}(0) \equiv \alpha_2 y_2(0) - \sqrt{\varepsilon}\beta_2 y_2'(0) = p_2, & \mathcal{R}_2^{(1)}\vec{y}(1) \equiv \gamma_2 y_2(1) + \sqrt{\varepsilon}\delta_2 y_2'(1) = q_2, \end{cases} \tag{1.3}$$

Uncorrected Proof

where $\alpha_i,\ \beta_i \geqslant 0,\ \alpha_i+\beta_i>0,\ \gamma_i>0,\ \delta_i \geqslant 0$ for $i=1,2$. For convenience, we introduce the notations $\boldsymbol{\mathcal{R}}^{(k)}\vec{y}(k) = \left(\mathcal{R}_1^{(k)}\vec{y}(k),\ \mathcal{R}_2^{(k)}\vec{y}(k)\right)$ for $k=0,1$, $P=(p_1,p_2)^T$ and $Q=(q_1,q_2)^T$. The objective is to find $y_1, y_2 \in C^0(\bar{D}) \cap C^4(D^- \cup D^+)$ such that (1.1) and (1.3) are satisfied. We assume that the coefficient functions satisfy

$$b_{ij}(t) \leqslant 0, \quad \text{when} \quad i \neq j \quad \text{and} \quad t \in D. \tag{1.4}$$

Additionally, we introduce the constant λ, which is defined as

$$0<\lambda<\min_{\bar{D}}\left\{\sum_{j=1}^{2} b_{1j}(t),\ \sum_{j=1}^{2} b_{2j}(t)\right\}, \quad 1 \leqslant j \leqslant 2. \tag{1.5}$$

Thus, $b_{11}(t) > |b_{12}(t)|$ and $b_{22}(t) > |b_{21}(t)|$ on $\bar{D}$. At the point of discontinuity, we assume $|f_1| \leqslant C$ and $|f_2| \leqslant C$, where C is a generic constant, a convention we adopt throughout this paper. The coefficient functions $b_{ij}(t) \in C^3(D)$ and source terms $f_i(t) \in C^2(D^- \cup D^+)$ for $1 \leqslant i,j \leqslant 2$. Moreover, the derivative bounds of these functions are considered independent of the singular perturbation parameter. We apply the hybrid scheme outlined by Das et al. [8] and obtain almost second-order $\varepsilon-$uniform convergence.

The paper is structured as follows: Section 2 examines the maximum principle, stability result, the components of the solution $\vec{y}$ and bounds on their derivatives. The construction of the mesh and the hybrid finite difference operator are described in Section 3. In Section 4, we establish that the numerical solution of (1.1), obtained using the method from Section 3, attains uniform convergence in the maximum norm with an order close to two. Section 5 presents numerical problems, which supports our theoretical results.

Uncorrected Proof

Notations

The maximum norm of a continuous real-valued function g defined on X is given by $\|g\|_X = \max_{t\in X}|g(t)|$. Suppose $\vec{g}(t) = (g_1(t), g_2(t))^T$ is a vector function, then $\|\vec{g}\|_X = \max\{\|g_1\|_X, \|g_2\|_X\}$. We define $\vec{g}(t) \leqslant \vec{h}(t)$, if for all t in $[0,1]$, the component-wise inequalities $g_1(t) \leqslant h_1(t)$ and $g_2(t) \leqslant h_2(t)$ holds. Furthermore, we write $\vec{g} \leqslant k$ to denote $\vec{g} \leqslant k(1,1)^T$, where k is a scalar. A mesh $D^N := \{t_i\}_{i=0}^N$ is a set of nodes such that $0=t_0<t_1<\ldots<t_N=1$. A real-valued function $\phi := \{\phi(t_i)\}_{i=0}^N$ defined on D^N is said to be a mesh function. The discrete maximum norm of a mesh function is defined by $\|\phi\|_{I^N} = \max_{i=0,1,\ldots,N}\|\phi(t_i)\|$. For vector mesh functions $\vec{\phi} := (\phi_1,\phi_2)^T = \{(\phi_1(t_i),\phi_2(t_i))\}_{i=0}^N$, the discrete maximum norm is $\|\vec{\phi}\|_{I^N} = \max\{\|\phi_1\|_{I^N}, \|\phi_2\|_{I^N}\}$.

2. A priori bounds on the solution and its derivatives

In this section, bounds are showed for the continuous solution and its derivatives. Error analysis is carried out by decomposing the solution into smooth and layer components. The differential operator $\mathbf{P}$ in (1.1) satisfies the following maximum principle for any $\vec{\psi} \in C^2(D^- \cup D^+)$. Stability follows as a direct consequence of this maximum principle. The proofs of these results can be obtained using arguments similar to those presented in [2, 5, 27].

Lemma 2.1. *(Maximum principle) Suppose that* $\boldsymbol{\mathcal{R}}^{(0)}\vec{\psi}(0) \geqslant 0$ *and* $\boldsymbol{\mathcal{R}}^{(1)}\vec{\psi}(1) \geqslant 0$. *Then* $\mathbf{P}\vec{\psi}(t) \geqslant 0$ *for* $t \in D^- \cup D^+$ *and* $[\vec{\psi}'](\eta) \leqslant 0$ *implies that* $\vec{\psi}(t) \geqslant 0$ *for all* $t \in \bar{D}$.

Lemma 2.2. *(Stability result) If* $\vec{y}$ *satisfies the system* (1.1)–(1.3), *then*

$$\|\vec{y}\|_{\bar{D}} \leqslant C \max\left\{\|\mathbf{P}\vec{y}\|_{D^-\cup D^+},\ \left\|\boldsymbol{\mathcal{R}}^{(0)}\vec{y}(0)\right\|,\ \left\|\boldsymbol{\mathcal{R}}^{(1)}\vec{y}(1)\right\|\right\},$$

where C *is a generic constant.*

Theorem 2.3 (Basha et al. [5])**.** *Suppose* $\vec{y}$ *is the solution of* (1.1) – (1.3), *then for* $k=0,1,\ldots,4$,

$$\left\|\vec{y}^{(k)}\right\| \leqslant C\left(1+\varepsilon^{-k/2}\right), \qquad t \in \bar{D}\setminus\{\eta\},$$

where C *is independent of perturbation parameter.*

Proof. The proof is first established for the case $k = 0$. Define the auxiliary functions

$$\vec{\psi}^{\pm}(t) = \left(\frac{1}{\lambda}\|\vec{f}\| + \max\left\{ \left\| \boldsymbol{\mathcal{R}}^{(0)}\vec{y}(0) \right\|, \ \left\| \boldsymbol{\mathcal{R}}^{(1)}\vec{y}(1) \right\| \right\} \right) (1,1)^T \pm \vec{y}(t),$$

for all $t \in \bar{D} \setminus \{\eta\}$. These functions satisfy

$$\boldsymbol{\mathcal{R}}^{(0)}\vec{\psi}(0) \geqslant 0, \qquad \boldsymbol{\mathcal{R}}^{(1)}\vec{\psi}(1) \geqslant 0,$$

together with

$$\mathbf{P}\vec{\psi}^{\pm}(t) = B(t) \begin{pmatrix} 1 \\ 1 \end{pmatrix} \frac{1}{\lambda}\|\vec{f}\| \pm \vec{f}(t) \geqslant 0.$$

Applying Lemma 2.1, it follows that $\vec{\psi}^{\pm}(t) \geqslant 0$, which yields

$$|\vec{y}(t)| \leqslant \frac{1}{\lambda}\|\vec{f}\| + \max\left\{ \left\| \boldsymbol{\mathcal{R}}^{(0)}\vec{y}(0) \right\|, \ \left\| \boldsymbol{\mathcal{R}}^{(1)}\vec{y}(1) \right\| \right\},$$

for all $t \in \bar{D} \setminus \{\eta\}$. Next, an estimate for the first derivative is derived. For any fixed $t \in \bar{D} \setminus \{\eta\}$, consider a neighbourhood $N_t = (a, a + \sqrt{\varepsilon})$ such that $t \in N_t$ and either $N_t \subset [0, \eta)$ or $N_t \subset (\eta, 1]$. By the Mean Value Theorem, there exists some $c \in \bar{N}_t$ satisfying

$$\frac{\vec{y}(a + \sqrt{\varepsilon}) - \vec{y}(a)}{\sqrt{\varepsilon}} = \vec{y}\,'(c).$$

Consequently,

$$|\vec{y}(c)| \leqslant 2\varepsilon^{-1/2}\|\vec{y}\,\|_{N_t} \leqslant C\varepsilon^{-1/2}.$$

Using the differential equation,

$$y_1'(t) = y_1'(c) + \int_c^t y_1''(s)ds = y_1'(c) + \varepsilon^{-1}\int_c^t \left(b_{11}y_1 + b_{12}y_2 - f_1\right)(s)ds,$$

which implies that $|y_1'(t)| \leqslant C\varepsilon^{-1/2}$. An analogous argument gives $|y_2'(t)| \leqslant C\varepsilon^{-1/2}$. Finally, the estimates for the higher-order derivatives follow directly from the governing differential equations together with the previously established bounds on $\vec{y}$ and $\vec{y}\,'$. □

To establish sharp bounds for the solution of singularly perturbed linear equations, the solution is written as a sum of smooth and layer components and an analysis is carried out on each component. The smooth part closely approximates the solution over most of the domain, with its lower derivatives bounded regardless of the perturbation parameter. The layer component, on the other hand, exhibits large first-order derivatives near the boundary but rapidly decreases towards the interior of the domain. We write (as given by Miller [24])

$$\vec{y} = \vec{r} + \vec{s}, \tag{2.1}$$

where $\vec{r} = (r_1, r_2)^T$ is the solution to

$$\begin{aligned}
&\mathbf{P}\vec{r} = \vec{f} \quad \text{on} \quad D^- \cup D^+, \\
&\boldsymbol{\mathcal{R}}^{(0)}\vec{r}(0) = B(0)^{-1}\vec{f}(0), \quad \boldsymbol{\mathcal{R}}^{(1)}\vec{r}(1) = B(1)^{-1}\vec{f}(1), \\
&\vec{r}(\eta^-) = B(\eta)^{-1}\vec{f}(\eta^-), \quad \vec{r}(\eta^+) = B(\eta)^{-1}\vec{f}(\eta^+),
\end{aligned}$$

and $\vec{s} = (s_1, s_2)^T$ satisfies

$$\begin{aligned}
&\mathbf{P}\vec{s} = \vec{0} \quad \text{on} \quad D^- \cup D^+, \\
&\boldsymbol{\mathcal{R}}^{(0)}\vec{s}(0) = P - \boldsymbol{\mathcal{R}}^{(0)}\vec{r}(0), \quad \boldsymbol{\mathcal{R}}^{(1)}\vec{s}(1) = Q - \boldsymbol{\mathcal{R}}^{(1)}\vec{r}(1), \\
&[\vec{s}\,](\eta) = [\vec{r}\,](\eta), \quad [\vec{s}\,'](\eta) = -[\vec{r}\,'](\eta),
\end{aligned}$$

Uncorrected Proof

and the matrix B is invertible since it satisfies (1.4) and (1.5). The layer functions

$$\mathbb{B}_l(t,\lambda) = \exp\left(-t\sqrt{\lambda/\varepsilon}\right) + \exp\left(-(\eta-t)\sqrt{\lambda/\varepsilon}\right);$$
$$\mathbb{B}_r(t,\lambda) = \exp\left(-(t-\eta)\sqrt{\lambda/\varepsilon}\right) + \exp\left(-(1-t)\sqrt{\lambda/\varepsilon}\right);$$

are defined on D^- and D^+ respectively. These functions are useful for establishing bounds on the derivatives of $\vec{r}$ and $\vec{s}$.

Lemma 2.4. *(Estimates for the smooth and layer components) If (2.1) holds, then for $0 \leqslant j \leqslant 4$,*

$$|\vec{r}^{(j)}| \leqslant C(1+\varepsilon^{-(j-2)/2}) \text{ on } D^- \cup D^+, \tag{2.2}$$

$$|\vec{s}^{(j)}| \leqslant \begin{cases} C\varepsilon^{-j/2}\mathbb{B}_l(x,\lambda) & \text{on } D^- \\ C\varepsilon^{-j/2}\mathbb{B}_r(x,\lambda) & \text{on } D^+. \end{cases} \tag{2.3}$$

Proof. Using the approach in [19], we derive (2.2) for $j = 0, 1, \ldots, 3$. The bound for $j = 4$ follows by differentiating $\mathbf{P}\vec{r} = \vec{f}$ twice and using lower-order estimates. Similarly, (2.3) is established for $j = 0, 1, 2$, while the bounds for $j = 3, 4$ follows by differentiating $\mathbf{P}\vec{s} = \vec{0}$ and applying lower-order derivative estimates. □

3. Discretization of the problem

This section presents the hybrid scheme (cf. [9], [12], [4]) on a piecewise−uniform Shishkin mesh, developed for solving (1.1) – (1.3). For further discussion on Shishkin mesh (see [11, 24, 29]). The subdomain D^- is partitioned into three piecewise−uniform subintervals: $[0,\sigma_1], [\sigma_1, \eta-\sigma_1]$ and $[\eta-\sigma_1, \eta]$, with uniform subdivisions of $N/8, N/4$ and $N/8$ intervals, respectively. Similarly, the subdomain D^+ is divided into $[\eta, \eta+\sigma_2], [\eta+\sigma_2, 1-\sigma_2]$ and $[1-\sigma_2, 1]$, again subdivided uniformly into $N/8, N/4$ and $N/8$ intervals. The transition parameters σ_1 and σ_2 are given by

$$\sigma_1 = \min\{\eta/4,\ \sigma_0\sqrt{\varepsilon}\ln N\} \quad \text{and} \quad \sigma_2 = \min\{(1-\eta)/4,\ \sigma_0\sqrt{\varepsilon}\ln N\},$$

with $\sigma_0 \geqslant 2/\sqrt{\lambda} > 0$. Moreover, the conditions $0 < \sigma_1 \leqslant \eta/4$ and $0 < \sigma_2 \leqslant (1-\eta)/4$, must be satisfied; otherwise, D^- and D^+ would result in a uniform mesh.

Let $\{t_k\}_{k=0}^N$ denote a general mesh. The step sizes are defined by $h_k = t_k - t_{k-1}$ for $1 \leqslant k \leqslant N$ and the average step sizes by $\hbar_k = (h_k + h_{k+1})/2$ for $1 \leqslant k \leqslant N-1$. The central difference operator is defined as

$$\delta^2\psi_k = \frac{1}{\hbar_k}\left(\frac{\psi_{k+1}-\psi_k}{h_{k+1}} - \frac{\psi_k - \psi_{k-1}}{h_k}\right),$$

which is applied to an arbitrary mesh function ψ_k. If $y(t)$ is known at the nodes $t_0, t_1, \ldots, t_N$ with corresponding values $y(t_0), y(t_1), \ldots, y(t_N)$, the cubic spline polynomial function $G(t)$ satisfies the following characteristics:

(i) The function $G(t)$ is identical to a cubic polynomial on $[t_j, t_{j+1}]$, for $0 \leqslant j \leqslant N$,
(ii) $G(t)$ belongs to $C^2(D^- \cup D^+)$,
(iii) $G(t_j) = y(t_j)$, where $0 \leqslant j \leqslant N$.

For a more detailed discussion on cubic spline interpolation, refer [8], [1] and [25]. On an arbitrary subinterval $[t_j, t_{j+1}]$, the cubic spline interpolating polynomial function is defined as,

$$\begin{cases} G(t) = \dfrac{(t_{j+1}-t)^3}{6h_{j+1}}M_j + \dfrac{(t-t_j)^3}{6h_{j+1}}M_{j+1} + \left(y(t_j) - \dfrac{h_{j+1}^2}{6}M_j\right)\left(\dfrac{t_{j+1}-t}{h_{j+1}}\right) \\ \qquad + \left(y(t_{j+1}) - \dfrac{h_{j+1}^2}{6}M_{j+1}\right)\left(\dfrac{t-t_j}{h_{j+1}}\right) \quad \text{for } 0 \leqslant j \leqslant N-1. \end{cases} \tag{3.1}$$

where $M_j = G''(t_j), \quad 0 \leqslant j \leqslant N$. The following one-sided limits, which we will use for approximating Robin boundary conditions can be derived from (3.1) as follows:

$$G^-(t_j) = \frac{h_j}{6}M_{j-1} + \frac{h_j}{3}M_j + \frac{y(t_j)-y(t_{j-1})}{h_j}, \tag{3.2}$$

Uncorrected Proof

$$G^+(t_j) = \frac{-h_{j+1}}{3}M_j - \frac{h_{j+1}}{6}M_{j+1} + \frac{y(t_{j+1}) - y(t_j)}{h_{j+1}}. \tag{3.3}$$

To satisfy point (ii), the function $G(t)$ must fulfil the following continuity condition:

$$\frac{h_j}{6}M_{j-1} + \left(\frac{h_j + h_{j+1}}{3}\right)M_j + \frac{h_{j+1}}{6}M_{j+1} = \frac{y(t_{j+1}) - y(t_j)}{h_{j+1}} - \frac{y(t_j) - y(t_{j-1})}{h_j},$$

for $1 \leqslant j \leqslant N-1$. Replace $G_{1,k}$ and $G_{2,k}$ from the following equations into the respective equations defined for y_1 and y_2 in (1.1) respectively.

$$-\varepsilon S_{1,k} + b_{11}(t_k)y_1(t_k) + b_{12}(t_k)y_2(t_k) = f_1(t_k), \quad k = j-1, j, j+1,$$
$$-\varepsilon S_{2,k} + b_{21}(t_k)y_1(t_k) + b_{22}(t_k)y_2(t_k) = f_2(t_k), \quad k = j-1, j, j+1.$$

The following set of linear equations will be obtained for $Y_{1,k}$ and $Y_{2,k}$ where $1 \leq k \leq N-1$.

$$\left[\frac{-3\varepsilon}{2h_j\hbar_j} + \frac{h_j b_{11}(t_{j-1})}{4\hbar_j}\right]Y_{1,j-1} + \left[\frac{3\varepsilon}{h_j h_{j+1}} + b_{11}(t_j)\right]Y_{1,j} + \left[\frac{-3\varepsilon}{2h_{j+1}\hbar_j} + \frac{h_{j+1}b_{11}(t_{j+1})}{4\hbar_j}\right]Y_{1,j+1}$$
$$+ \left[\frac{h_j b_{12}(t_{j-1})}{4\hbar_j}\right]Y_{2,j-1} + [b_{12}(t_j)]\,Y_{2,j} + \left[\frac{h_{j+1}b_{12}(t_{j+1})}{4\hbar_j}\right]Y_{2,j+1}$$
$$= \left[\frac{h_j}{4\hbar_j}\right]f_1(t_{j-1}) + f_1(t_j) + \left[\frac{h_{j+1}}{4\hbar_j}\right]f_1(t_{j+1}).$$

$$\left[\frac{-3\varepsilon}{2h_j\hbar_j} + \frac{h_j b_{22}(t_{j-1})}{4\hbar_j}\right]Y_{2,j-1} + \left[\frac{3\varepsilon}{h_j h_{j+1}} + b_{22}(t_j)\right]Y_{2,j} + \left[\frac{-3\varepsilon}{2h_{j+1}\hbar_j} + \frac{h_{j+1}b_{22}(t_{j+1})}{4\hbar_j}\right]Y_{2,j+1}$$
$$+ \left[\frac{h_j b_{21}(t_{j-1})}{4\hbar_j}\right]Y_{1,j-1} + [b_{21}(t_j)]\,Y_{1,j} + \left[\frac{h_{j+1}b_{21}(t_{j+1})}{4\hbar_j}\right]Y_{1,j+1}$$
$$= \left[\frac{h_j}{4\hbar_j}\right]f_2(t_{j-1}) + f_2(t_j) + \left[\frac{h_{j+1}}{4\hbar_j}\right]f_2(t_{j+1}).$$

By applying the one - sided limits (3.2) and (3.3), we discretize the Robin boundary conditions (1.3) and derive the following equations:

$$\left[\frac{3\varepsilon}{h_1}(\alpha_1 + \frac{\beta_1}{h_1}) + b_{11}(t_0)\beta_1\right]Y_{1,0} + \left[\frac{-3\varepsilon\beta_1}{h_1^2} + \frac{b_{11}(t_1)\beta_1}{2}\right]Y_{1,1} + [b_{12}(t_0)\beta_1]\,Y_{2,0} + \left[\frac{\beta_1 b_{12}(t_1)}{2}\right]Y_{2,1}$$
$$= \frac{3\varepsilon p_1}{h_1} + \beta_1 f_1(t_0) + \frac{\beta_1 f_1(t_1)}{2},$$
$$\left[\frac{-3\varepsilon\delta_1}{h_N^2} + \frac{b_{11}(t_{N-1})\delta_1}{2}\right]Y_{1,N-1} + \left[\frac{3\varepsilon}{h_N}\left(\gamma_1 + \frac{\delta_1}{h_N}\right) + b_{11}(t_N)\delta_1\right]Y_{1,N} + \left[\frac{\delta_1 b_{12}(t_{N-1})}{2}\right]Y_{2,N-1} + [b_{12}(t_N)\delta_1]\,Y_{2,N}$$
$$= \frac{3\varepsilon q_1}{h_N} + \frac{\delta_1 f_1(t_{N-1})}{2} + \delta_1 f_1(t_N)$$
$$\left[\frac{3\varepsilon}{h_1}(\alpha_2 + \frac{\beta_2}{h_1}) + b_{22}(t_0)\beta_2\right]Y_{2,0} + \left[\frac{-3\varepsilon\beta_2}{h_1^2} + \frac{b_{22}(t_1)\beta_2}{2}\right]Y_{2,1} + [b_{21}(t_0)\beta_2]\,Y_{1,0} + \left[\frac{\beta_2 b_{21}(t_1)}{2}\right]Y_{1,1}$$
$$= \frac{3\varepsilon p_2}{h_1} + \beta_2 f_2(t_0) + \frac{\beta_2 f_2(t_1)}{2}.$$
$$\left[\frac{-3\varepsilon\delta_2}{h_N^2} + \frac{b_{22}(t_{N-1})\delta_2}{2}\right]Y_{2,N-1} + \left[\frac{3\varepsilon}{h_N}\left(\gamma_2 + \frac{\delta_2}{h_N}\right) + b_{22}(t_N)\delta_2\right]Y_{2,N} + \left[\frac{\delta_2 b_{21}(t_{N-1})}{2}\right]Y_{1,N-1} + [b_{21}(t_N)\delta_2]\,Y_{1,N}$$

Uncorrected Proof

$$= \frac{3\varepsilon q_2}{h_N} + \frac{\delta_2 f_2(t_{N-1})}{2} + \delta_2 f_2(t_N).$$

Define $D^N = D_N^- \cup D_N^+$, where $D_N^- = \{t_j : 0 < j < N/2\}$ and $D_N^+ = \{t_j : N/2 < j < N\}$. The discrete version of the continuous problem (1.1) is given by

$$\mathbf{P}^N \vec{Y} \equiv \begin{pmatrix} P_1^N \vec{Y} \\ P_2^N \vec{Y} \end{pmatrix} = \begin{pmatrix} F_1 \\ F_2 \end{pmatrix}.$$

Hence for $j = 1, \ldots, N-1$,

$$\begin{cases} P_1^N \vec{Y} \equiv A_{1,j}^- Y_{1,j-1} + A_{1,j}^c Y_{1,j} + A_{1,j}^+ Y_{1,j+1} + B_{1,j}^- Y_{2,j-1} + B_{1,j}^c Y_{2,j} + B_{1,j}^+ Y_{2,j+1}, \\ P_2^N \vec{Y} \equiv A_{2,j}^- Y_{1,j-1} + A_{2,j}^c Y_{1,j} + A_{2,j}^+ Y_{1,j+1} + B_{2,j}^- Y_{2,j-1} + B_{2,j}^c Y_{2,j} + B_{2,j}^+ Y_{2,j+1}, \\ F_1^N \equiv F_{1,j}^- f_{1,j-1} + F_{1,j}^c f_{1,j} + F_{1,j}^+ f_{1,j+1}, \\ F_2^N \equiv F_{2,j}^- f_{2,j-1} + F_{2,j}^c f_{2,j} + F_{2,j}^+ f_{2,j+1}. \end{cases} \tag{3.4}$$

The continuous Robin boundary conditions (1.3) in discrete form are

$$\boldsymbol{\mathcal{R}}^{N,(0)} \vec{Y}_0 = \left(\mathcal{R}_1^{N,(0)} \vec{Y}_0,\ \mathcal{R}_2^{N,(0)} \vec{Y}_0 \right), \qquad \boldsymbol{\mathcal{R}}^{N,(1)} \vec{Y}_N = \left(\mathcal{R}_1^{N,(1)} \vec{Y}_N,\ \mathcal{R}_2^{N,(1)} \vec{Y}_N \right), \tag{3.5}$$

where

$$\mathcal{R}_1^{N,(0)} \vec{Y}_0 \equiv \alpha_1 Y_{1,0} - \sqrt{\varepsilon}\beta_1 G^+(Y_{1,0}) = p_1, \qquad \mathcal{R}_1^{N,(1)} \vec{Y}_N \equiv \gamma_1 Y_{1,N} + \sqrt{\varepsilon}\delta_1 G^-(Y_{1,N}) = q_1,$$
$$\mathcal{R}_2^{N,(0)} \vec{Y}_0 \equiv \alpha_2 Y_{2,0} - \sqrt{\varepsilon}\beta_2 G^+(Y_{2,0}) = p_2, \qquad \mathcal{R}_2^{N,(1)} \vec{Y}_N \equiv \gamma_2 Y_{2,N} + \sqrt{\varepsilon}\delta_2 G^-(Y_{2,N}) = q_2.$$

For $1 \leqslant j \leqslant N/8 - 1$ the discretization follows:

$$\begin{cases} A_{1,j}^- = \dfrac{-3\varepsilon}{2h_j\hbar_j} + \dfrac{h_j b_{11}(t_{j-1})}{4\hbar_j}; \quad A_{1,j}^c = \dfrac{3\varepsilon}{h_j h_{j+1}} + b_{11}(t_j); \quad A_{1,j}^+ = \dfrac{-3\varepsilon}{2h_{j+1}\hbar_j} + \dfrac{h_{j+1} b_{11}(t_{j+1})}{4\hbar_j}; \\ B_{1,j}^- = \dfrac{h_j b_{12}(t_{j-1})}{4\hbar_j}; \quad B_{1,j}^c = b_{12}(t_j); \quad B_{1,j}^+ = \dfrac{h_{j+1} b_{12}(t_{j+1})}{4\hbar_j}; \\ F_{1,j}^- = \dfrac{h_j}{4\hbar_j}; \quad F_{1,j}^c = 1; \quad F_{1,j}^+ = \dfrac{h_{j+1}}{4\hbar_j}; \\ A_{2,j}^- = \dfrac{h_j b_{21}(t_{j-1})}{4\hbar_j}; \quad A_{2,j}^c = b_{21}(t_j); \quad A_{2,j}^+ = \dfrac{h_{j+1} b_{21}(t_{j+1})}{4\hbar_j}; \\ B_{2,j}^- = \dfrac{-3\varepsilon}{2h_j\hbar_j} + \dfrac{h_j b_{22}(t_{j-1})}{4\hbar_j}; \quad B_{2,j}^c = \dfrac{3\varepsilon}{h_j h_{j+1}} + b_{22}(t_j); \quad B_{2,j}^+ = \dfrac{-3\varepsilon}{2h_{j+1}\hbar_j} + \dfrac{h_{j+1} b_{22}(t_{j+1})}{4\hbar_j}; \\ F_{2,j}^- = \dfrac{h_j}{4\hbar_j}; \quad F_{2,j}^c = 1; \quad F_{2,j}^+ = \dfrac{h_{j+1}}{4\hbar_j}. \end{cases}$$

The same discretization is used for $7N/8 + 1 \leqslant j \leqslant N - 1$. For the remaining intervals the discretization follows accordingly, ensuring a consistent numerical approach to resolve layers and discontinuities. For $N/8 \leqslant j \leqslant N/2 - 1$ and $N/2 + 1 \leqslant j \leqslant 7N/8$, the coefficients are defined as,

$$\begin{cases} A_{1,j}^- = \dfrac{-\varepsilon}{h_j\hbar_j}; \quad A_{1,j}^c = \dfrac{2\varepsilon}{h_j h_{j+1}} + b_{11}(t_j); \quad A_{1,j}^+ = \dfrac{-\varepsilon}{h_{j+1}\hbar_j}; \\ B_{1,j}^- = 0; \quad B_{1,j}^c = b_{12}(t_j); \quad B_{1,j}^+ = 0; \\ F_{1,j}^- = 0; \quad F_{1,j}^c = 1; \quad F_{1,j}^+ = 0; \\ A_{2,j}^- = 0; \quad A_{2,j}^c = b_{21}(t_j); \quad A_{2,j}^+ = 0; \\ B_{2,j}^- = \dfrac{-\varepsilon}{h_j\hbar_j}; \quad B_{2,j}^c = \dfrac{2\varepsilon}{h_j h_{j+1}} + b_{22}(t_j); \quad B_{2,j}^+ = \dfrac{-\varepsilon}{h_{j+1}\hbar_j}; \\ F_{2,j}^- = 0; \quad F_{2,j}^c = 1; \quad F_{2,j}^+ = 0. \end{cases} \tag{3.6}$$

Uncorrected Proof

For $j = N/2$, the coefficients are the same as in Equation (3.6), except for the following.

$$\begin{cases} F^-_{1,N/2} = 1/2; \quad F^c_{1,N/2} = 0; \quad F^+_{1,N/2} = 1/2; \\ F^-_{2,N/2} = 1/2; \quad F^c_{2,N/2} = 0; \quad F^+_{2,N/2} = 1/2. \end{cases}$$

For $j = 0$ (discretization of Robin boundary conditions),

$$\begin{cases} A^c_{1,0} = \dfrac{3\varepsilon}{h_1}\left(\alpha_1 + \dfrac{\beta_1}{h_1}\right) + b_{11}(t_0)\beta_1; \quad A^+_{1,0} = \dfrac{-3\varepsilon\beta_1}{h_1^2} + \dfrac{b_{11}(t_1)\beta_1}{2}; \\ B^c_{1,0} = \beta_1 b_{12}(t_0); \quad B^+_{1,0} = \dfrac{\beta_1 b_{12}(t_1)}{2}; \\ F^-_{1,0} = \dfrac{3\varepsilon p_1}{h_1}; \quad F^c_{1,0} = \beta_1; \quad F^+_{1,0} = \dfrac{\beta_1}{2}; \\ A^c_{2,0} = \beta_2 b_{21}(t_0); \quad A^+_{2,0} = \dfrac{\beta_2 b_{21}(t_1)}{2}; \\ B^c_{2,0} = \dfrac{3\varepsilon}{h_1}\left(\alpha_2 + \dfrac{\beta_2}{h_1}\right) + b_{22}(t_0)\beta_2; \quad B^+_{2,0} = \dfrac{-3\varepsilon\beta_2}{h_1^2} + \dfrac{b_{22}(t_1)\beta_2}{2}; \\ F^-_{2,0} = \dfrac{3\varepsilon p_2}{h_1}; \quad F^c_{2,0} = \beta_2; \quad F^+_{2,0} = \dfrac{\beta_2}{2}. \end{cases}$$

For $j = N$,

$$\begin{cases} A^-_{1,N} = \dfrac{-3\varepsilon\delta_1}{h_N^2} + \dfrac{b_{11}(t_{N-1})\delta_1}{2}; \quad A^c_{1,N} = \dfrac{3\varepsilon}{h_N}\left(\gamma_1 + \dfrac{\delta_1}{h_N}\right) + b_{11}(t_N)\delta_1; \\ B^-_{1,N} = \dfrac{\delta_1 b_{12}(t_{N-1})}{2}; \quad B^c_{1,N} = b_{12}(t_N)\delta_1; \\ F^-_{1,N} = \dfrac{\delta_1}{2}; \quad F^c_{1,N} = \delta_1; \quad F^+_{1,N} = \dfrac{3\varepsilon q_1}{h_N}; \\ A^-_{2,N} = \dfrac{\delta_2 b_{21}(t_{N-1})}{2}; \quad A^c_{2,N} = b_{21}(t_N)\delta_2; \\ B^-_{2,N} = \dfrac{-3\varepsilon\delta_2}{h_N^2} + \dfrac{b_{22}(t_{N-1})\delta_2}{2}; \quad B^c_{2,N} = \dfrac{3\varepsilon}{h_N}\left(\gamma_2 + \dfrac{\delta_2}{h_N}\right) + b_{22}(t_N)\delta_2; \\ F^-_{2,N} = \dfrac{\delta_2}{2}; \quad F^c_{2,N} = \delta_2; \quad F^+_{2,N} = \dfrac{3\varepsilon q_2}{h_N}; \end{cases}$$

The discrete operator in (3.4), denoted by $\mathbf{P}^N = \left(P_1^N,\ P_2^N\right)^T$, satisfies the discrete maximum principle, from which stability follows. The corresponding results can be found in [5, 6].

Lemma 3.1. *(Discrete maximum principle) Consider a vector-valued mesh function $\{\vec{Y}(t_j)\}_{j=0}^N$ that satisfies $\boldsymbol{\mathcal{R}}^{N,(0)}\vec{Y}(t_0) \geqslant \vec{0}$ and $\boldsymbol{\mathcal{R}}^{N,(1)}\vec{Y}(t_N) \geqslant \vec{0}$. If $\mathbf{P}^N\vec{Y}(t_j) \geqslant 0$ for all $1 \leqslant j \leqslant N-1$, then it follows that $\vec{Y}(t_j) \geqslant 0$ for all $0 \leqslant j \leqslant N$.*

Lemma 3.2. *(Discrete stability result) If $\vec{Y}$ is any mesh function satisfying (3.4)–(3.5), then*

$$\left\|\vec{Y}\right\|_{D^N} \leqslant C \max\left\{\left\|\mathbf{P}^N\vec{Y}\right\|_{D_N^- \cup D_N^+},\ \left\|\boldsymbol{\mathcal{R}}^{N,(0)}\vec{Y}(0)\right\|,\ \left\|\boldsymbol{\mathcal{R}}^{N,(1)}\vec{Y}(1)\right\|\right\},$$

where C is a generic constant.

We decompose the numerical solution $\vec{Y}$ similar to the continuous solution (2.1) as $\vec{Y} = \vec{R} + \vec{S}$, where $\vec{R}$ is the solution to

$$\begin{aligned} &\mathbf{P}^N\vec{R} = \vec{F}(t_j), \quad \text{on} \quad D_N^- \cup D_N^+, \\ &\boldsymbol{\mathcal{R}}^{N,(0)}\vec{R}(0) = \boldsymbol{\mathcal{R}}^{(0)}\vec{r}(0), \quad \boldsymbol{\mathcal{R}}^{N,(1)}\vec{R}(1) = \boldsymbol{\mathcal{R}}^{(1)}\vec{r}(1), \\ &\vec{R}(\eta) = \vec{r}(\eta), \end{aligned}$$

Uncorrected Proof

and $\vec{S}$ is the solution to

$$\begin{aligned}
&\mathbf{P}^N \vec{S} = \vec{0}, \quad \text{on} \quad D_N^- \cup D_N^+, \\
&\boldsymbol{\mathcal{R}}^{N,(0)} \vec{S}(0) = \boldsymbol{\mathcal{R}}^{(0)} \vec{s}(0), \quad \boldsymbol{\mathcal{R}}^{N,(1)} \vec{S}(1) = \boldsymbol{\mathcal{R}}^{(1)} \vec{s}(1), \\
&[\vec{S}](\eta) = -[\vec{R}](\eta), \quad [D\vec{S}](\eta) = -[D\vec{R}](\eta),
\end{aligned}$$

where the discrete derivative in the mesh function $\vec{Y}$ exhibits a jump at $t_i = \eta$, which is defined by the condition $D^+\vec{Y}(\eta) = D^-\vec{Y}(\eta)$.
The next section provides a detailed analysis demonstrating the robustness and reliability of the given method.

4. Error estimates for the numerical method

This section focuses on the truncation error and the stability properties of the numerical scheme. We conclude by stating our primary result - the uniform convergence result. Based on the previously introduced piecewise−uniform mesh, the truncation error for the proposed scheme is derived as follows (see [8]):
Truncation error for $1 \leqslant j \leqslant N/8 - 1$ and $7N/8 - 1 \leqslant j \leqslant N - 1$,

$$\begin{cases}
\mathcal{T}_{j,y_1} &= \dfrac{\varepsilon h^2}{8} y_1^{(4)}(t_j) + A_{1,j}^+ T_4(t_j, t_{j+1}, y_1) + A_{1,j}^- T_4(t_j, t_{j-1}, y_1) \\
&\quad + \dfrac{\varepsilon}{4} T_2(t_j, t_{j+1}, y_1) + \dfrac{\varepsilon}{4} T_2(t_j, t_{j-1}, y_1) \\
&\quad - \dfrac{b_{11}(t_{j-1})}{4} T_4(t_j, t_{j-1}, y_1) - \dfrac{b_{11}(t_{j+1})}{4} T_4(t_j, t_{j+1}, y_1).
\end{cases}$$

$$\begin{cases}
\mathcal{T}_{j,y_2} &= \dfrac{\varepsilon h^2}{8} y_2^{(4)}(t_j) + A_{2,j}^+ T_4(t_j, t_{j+1}, y_2) + A_{2,j}^- T_4(t_j, t_{j-1}, y_2) \\
&\quad + \dfrac{\varepsilon}{4} T_2(t_j, t_{j+1}, y_2) + \dfrac{\varepsilon}{4} T_2(t_j, t_{j-1}, y_2) \\
&\quad - \dfrac{b_{22}(t_{j-1})}{4} T_4(t_j, t_{j-1}, y_2) - \dfrac{b_{22}(t_{j+1})}{4} T_4(t_j, t_{j+1}, y_2).
\end{cases}$$

In this expression, $\mathcal{T}_{j,u}$ represents the truncation error at t_j, h denotes the step size and $T_n(t, k, u)$ is the remainder resulting from the Taylor series expansion of u. For $N/8 \leqslant j \leqslant N/2 - 1$ and $N/2 + 1 \leqslant j \leqslant 7N/8$, it holds

$$\begin{cases}
\mathcal{T}_{j,y_1} = -\varepsilon \left(\delta^2 - \dfrac{d^2}{dt^2} \right) y_1(t_j), \\
\mathcal{T}_{j,y_2} = -\varepsilon \left(\delta^2 - \dfrac{d^2}{dt^2} \right) y_2(t_j).
\end{cases} \tag{4.1}$$

Since $y_1, y_2 \in C^3\left(D^- \cup D^+\right)$, it is well known that at $j = N/8$ and $7N/8$, it holds

$$\begin{aligned}
&|\mathcal{T}_{j,y_1}| \leqslant C\varepsilon \hbar_j \left| y_1^{(3)}(t_j) \right|, \\
&|\mathcal{T}_{j,y_2}| \leqslant C\varepsilon \hbar_j \left| y_2^{(3)}(t_j) \right|.
\end{aligned}$$

At $j = 0$, the truncation error is given by,

$$\mathcal{T}_{0,y_1} = A_{1,0}^c y_{1,0} + A_{1,0}^+ y_{1,1} + B_{1,0}^c y_{2,0} + B_{1,0}^+ y_{2,1} - F_{1,0}^- - F_{1,0}^c f_{1,0} - F_{1,0}^+ f_{1,1}.$$

Using the Taylor's theorem and Equation (1.1), we obtain

$$\mathcal{T}_{0,y_1} = T_{0,0} y_1(t_0) + T_{1,0} y_1^{(1)}(t_0) + T_{2,0} y_1^{(2)}(t_0) + T_{3,0} y_1^{(3)}(t_0) + T_{4,0} y_1^{(4)}(\xi),$$

where $\xi \in (0, 1)$. Here $T_{i,j}$ denotes the coefficients in the Taylor series expansion of the i^{th} derivative term at the point t_j. The coefficients are defined as follows (cf. [8]):

$$T_{0,0} = A_{1,0}^c + A_{1,0}^+ - \frac{3\varepsilon\alpha_1}{h_1} - F_{1,0}^c b_{11}(t_0) - F_{1,0}^+ b_{11}(t_1),$$

Uncorrected Proof

$$T_{1,0} = h_1 A^+_{1,0} + \frac{3\varepsilon\beta_1}{h_1} - \frac{\beta_1 b_{11}(t_1)h_1}{2},$$
$$T_{2,0} = \frac{h_1^2 A^+_{1,0}}{2} + \varepsilon\left(F^c_{1,0} + F^+_{1,0}\right) - \frac{h_1^2 F^+_{1,0} b_{11}(t_1)}{2},$$
$$T_{3,0} = \frac{h_1^3 A^+_{1,0}}{3!} + \varepsilon h_1 F^+_{1,0} - \frac{F^+_{1,0} b_{11}(t_1) h_1^3}{3!},$$
$$T_{4,0} = \frac{h_1^4 A^+_{1,0}}{4!} + \frac{\varepsilon h_1^2 F^+_{1,0}}{2} - \frac{F^+_{1,0} b_{11}(t_1) h_1^4}{4!}.$$

From these expressions, we obtain the following conditions:

$$T_{0,0} y_1(t_0) + T_{1,0} y_1^{(1)}(t_0) = 0, \quad T_{2,0} = 0, \quad T_{3,0} = 0, \quad T_{4,0} = \frac{7}{24}\varepsilon\beta_1 h_1^2.$$

The following bounds are satisfied at t_0 and t_N for y_1 and y_2:

$$|\mathcal{T}_{0,y_1}| \leqslant C\varepsilon\beta_1 h_1^2 |y^{(4)}_{1,0}|_{(t_0,t_1)}, \qquad |\mathcal{T}_{N,y_1}| \leqslant C\varepsilon\delta_1 h_N^2 |y^{(4)}_{1,N}|_{(t_{N-1},t_N)},$$
$$|\mathcal{T}_{0,y_2}| \leqslant C\varepsilon\beta_2 h_1^2 |y^{(4)}_{2,0}|_{(t_0,t_1)}, \qquad |\mathcal{T}_{N,y_2}| \leqslant C\varepsilon\delta_2 h_N^2 |y^{(4)}_{2,N}|_{(t_{N-1},t_N)}.$$

Next we analyze the pointwise errors by applying the Shishkin decomposition within each subinterval and proceed to the key result of this paper.

Theorem 4.1. *Let $\vec{y}$ denote the continuous solution of (1.1)–(1.3) and let $\vec{Y}$ represent the numerical solution obtained from the proposed scheme (3.4)–(3.5). Then the error at the discrete points satisfies*

$$\left\|\vec{y}(t_i) - \vec{Y}(t_i)\right\| \leqslant C\left(N^{-2}\ln^2 N + N^{-\sigma_0\sqrt{\lambda}}\right), \quad 0 \leqslant i \leqslant N.$$

Proof. Define the barrier function $\vec{\Psi} = (\Psi_1, \Psi_2)^T$ as

$$\vec{\Psi}(t_j) = C\left(N^{-2}\ln^2 N + N^{-\sigma_0\sqrt{\lambda}} + N^{-2}\frac{\sigma^2}{\sqrt{\varepsilon}}\Gamma(t_j)\right)\begin{pmatrix}1\\1\end{pmatrix}, \quad j = 1, \ldots, N-1,$$

where $\sigma = \sigma_1 = \sigma_2$ and the function $\Gamma(t_j)$ as

$$\Gamma(t_j) = \begin{cases} t, /\sigma & 0 \leqslant t \leqslant \sigma, \\ 1, & \sigma \leqslant t \leqslant 1-\sigma, \\ (1-t)/\sigma, & 1-\sigma \leqslant t \leqslant 1. \end{cases}$$

It follows that

$$\begin{aligned} P_1^N \vec{\Psi} \geqslant\ & C\left(N^{-2}\ln^2 N + N^{-\sigma_0\sqrt{\lambda}}\right)\left(A^-_{1,j} + A^c_{1,j} + A^+_{1,j} + B^-_{1,j} + B^c_{1,j} + B^+_{1,j}\right) \\ & + \frac{C\sigma^2 N^{-2}}{\sqrt{\varepsilon}}\Big(\left(A^-_{1,j} + B^-_{1,j} + A^-_{2,j} + B^-_{2,j}\right)\Gamma_{j-1} \\ & + \left(A^c_{1,j} + B^c_{1,j} + A^c_{2,j} + B^c_{2,j}\right)\Gamma_j + \left(A^+_{1,j} + B^+_{1,j} + A^+_{2,j} + B^+_{2,j}\right)\Gamma_{j+1}\Big). \end{aligned}$$

Case 1. For $0 \leqslant j \leqslant N/8 - 1$, the step size is given by $h = 8N^{-1}\sigma_0\sqrt{\varepsilon}\ln N$. By applying the solution decomposition (2.1) and using Lemma 2.4, we derive the estimate

$$|\mathbf{P}^N(\vec{Y} - \vec{y})(t_j)| \leqslant C\varepsilon h^2 |\vec{y}^{(4)}| \leqslant C\sigma_0^2 N^{-2}\ln^2 N. \tag{4.2}$$

A similar argument applies to the case $7N/8 + 1 \leqslant j \leqslant N$ (Refer [16] and [8] for details).

Case 2. From (4.1), for $N/8 + 1 \leqslant j \leqslant 3N/8 - 1$, we have

$$|\mathbf{P}^N(\vec{Y} - \vec{y})(t_j)| \leqslant \varepsilon\left|\left(\delta^2 - \frac{d^2}{dt^2}\right)\vec{r}(t_j)\right| + \varepsilon\left|\left(\delta^2 - \frac{d^2}{dt^2}\right)\vec{s}(t_j)\right|.$$

Uncorrected Proof

Since $h = 4N^{-1}\,(d - 2\sigma_0\sqrt{\varepsilon}\ln N)$ within the interval $(\sigma_1, d-\sigma_1)$, Lemma 2.4 implies that

$$\varepsilon\left|\left(\delta^2 - \frac{d^2}{dt^2}\right)\vec{r}(t_j)\right| \leqslant C\varepsilon h^2\left|\vec{r}^{(4)}\right| \leqslant CN^{-2}.$$

Moreover, by employing the arguments presented in [8], we deduce that

$$\varepsilon\left|\left(\delta^2 - \frac{d^2}{dt^2}\right)\vec{s}(t_j)\right| \leqslant CN^{-\sigma_0\sqrt{\lambda}}.$$

Thus,

$$|\mathbf{P}^N(\vec{Y} - \vec{y})(t_j)| \leqslant CN^{-\sigma_0\sqrt{\lambda}}. \tag{4.3}$$

A analogous argument applies for the case $5N/8 + 1 \leqslant j \leqslant 7N/8 - 1$.

Case 3. For $3N/8 + 1 \leqslant N/2 - 1$, from Miller [24], it can be shown that,

$$|\mathbf{P}^N(\vec{Y} - \vec{y})(t_j)| \leqslant C(N^{-1}\ln N)^2. \tag{4.4}$$

A similar result is applicable for $N/2 + 1 \leqslant 5N/8 - 1$.

Case 4. For $j = N/8$, $3N/8$, $5N/8$ and $7N/8$, we have $\hbar_j \leqslant 8\sigma_0\sqrt{\varepsilon}N^{-1}\ln N$. By applying Lemma 2.4, it follows that

$$\varepsilon\left|\left(\delta^2 - \frac{d^2}{dt^2}\right)\vec{r}(t_j)\right| \leqslant C\varepsilon\hbar_j\left|\vec{r}^{(3)}\right| \leqslant C\sqrt{\varepsilon}N^{-1}.$$

Using a similar argument, we obtain

$$\varepsilon\left|\left(\delta^2 - \frac{d^2}{dt^2}\right)\vec{s}(t_j)\right| \leqslant C(N^{-1} + N^{-\sigma_0\sqrt{\lambda}}).$$

It follows that

$$|\mathbf{P}^N(\vec{Y} - \vec{y})(t_j)| \leqslant C(N^{-1} + N^{-\sigma_0\sqrt{\lambda}}). \tag{4.5}$$

Case 5. For the case $j = N/2$, the argument presented in [10] applies. In this case,

$$|\mathbf{P}^N(\vec{Y} - \vec{y})(t_{N/2})| \leqslant C(N^{-1} + N^{-\sigma_0\sqrt{\lambda}}). \tag{4.6}$$

Applying the error bounds from case (1) – (5), we obtain

$$|P_1^N(\vec{y} - \vec{Y})| \leqslant |P_1^N\vec{\Psi}|.$$

Similarly, it can be shown that $\|P_2^N(\vec{y} - \vec{Y})\| \leqslant \|P_2^N\vec{\Psi}\|$. It follows from (4.2) – (4.6) that the matrix corresponding to the operator $\mathbf{P}^N$ is uniformly bounded. Consequently, the error estimate

$$\|\vec{y} - \vec{Y}\| \leqslant \|\vec{\Psi}\| \leqslant C(N^{-2}\ln^2 N + N^{-\sigma_0\sqrt{\lambda}}),$$

is established, since the inverse of the discrete operator $\mathbf{P}^N$ is $\varepsilon-$uniformly bounded. □

5. Numerical results

To validate the results of Section 4, two numerical examples are presented in this section. All computations were performed using MATLAB R2024b.

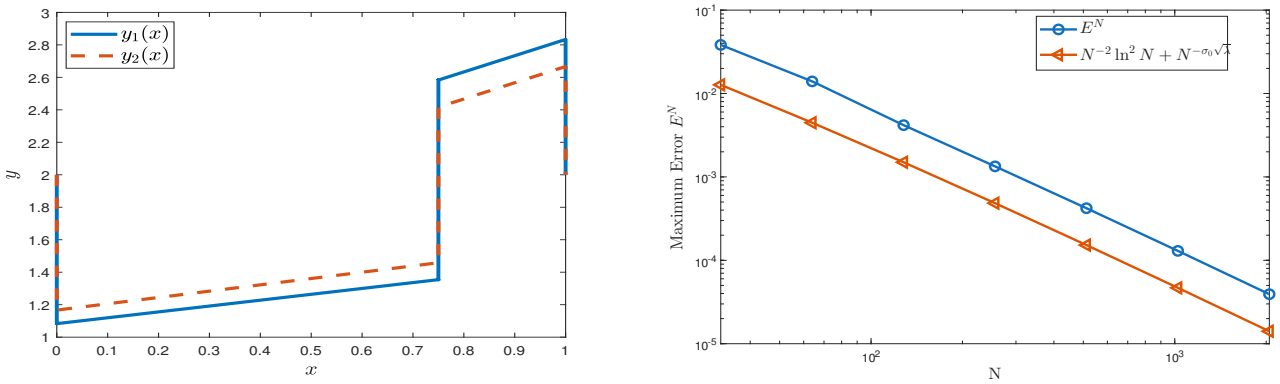
Example 5.1 (Constant coefficients)**.** Consider the coupled singularly perturbed reaction-diffusion system of the form (1.1), together with the Robin boundary conditions (1.3). Find $y = (y_1, y_2)$ satisfying

$$-\varepsilon y_1'' + 2y_1 - y_2 = f_1(t),$$
$$-\varepsilon y_2'' - 4y_1 + 5y_2 = f_2(t);$$

where,

$$f_1(t) = \begin{cases}(3+t)/3; & 0 \leqslant t \leqslant 3/4;\\ 2+t; & 3/4 < t \leqslant 1;\end{cases} \qquad f_2(t) = \begin{cases}(3+t)/2; & 0 \leqslant t \leqslant 3/4;\\ 1+t; & 3/4 < t \leqslant 1.\end{cases}$$

Uncorrected Proof



(A) Solution of Example 5.1 with $\varepsilon = 10^{-10}$ and $N = 128$.

(B) log – log plot of Example 5.1.

FIGURE 1. Example 5.1.

The system is subject to the Robin boundary conditions

$$y_1(0) - \sqrt{\varepsilon}y_1'(0) = 2; \qquad y_1(1) + \sqrt{\varepsilon}y_1'(1) = 2;$$
$$y_2(0) - \sqrt{\varepsilon}y_2'(0) = 2; \qquad y_2(1) + \sqrt{\varepsilon}y_2'(1) = 2.$$

The point of discontinuity is taken to be $d = 3/4$.

A plot of a typical solution to this problem is shown in Figure 1a. From this, it is clear that there are boundary layers near each of the boundaries $x = 0$ and $x = 1$, as well as the interior layer at $x = 3/4$. The boundary layers arise due to the small diffusion parameter, while the interior layer at $x = 3/4$ is caused by the nonsmooth source term. Such layer phenomena commonly appear in premixed combustion problems, where sharp temperature or concentration gradients develop near boundaries and reaction fronts (see [17] for more details).

Example 5.2 (Variable coefficients)**.** We solve

$$-\varepsilon y_1'' + 2(t+1)^2 y_1 - (1+t^3)y_2 = f_1(t),$$
$$-\varepsilon y_2'' - 2\cos\left(\frac{\pi t}{4}\right) y_1 + 2.2\exp(1-t)y_2 = f_2(t);$$

where,

$$f_1(t) = \begin{cases} 2e^t; & 0 \leqslant t \leqslant 1/2; \\ 1; & 1/2 < t \leqslant 1; \end{cases} \qquad f_2(t) = \begin{cases} 10t+1; & 0 \leqslant t \leqslant 1/2; \\ 2; & 1/2 < t \leqslant 1; \end{cases}$$

again with Robin boundary conditions

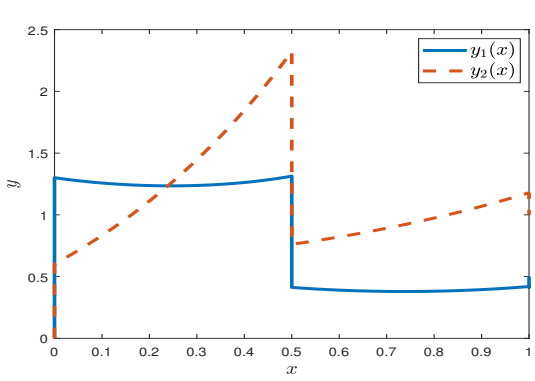
$$y_1(0) - \sqrt{\varepsilon}y_1'(0) = 0; \qquad 2y_1'(1) + \sqrt{\varepsilon}y_1'(1) = 1;$$
$$y_2(0) - 3\sqrt{\varepsilon}y_2'(0) = 0; \qquad y_2(1) + \sqrt{\varepsilon}y_2'(1) \ = 1,$$

corresponding to Equations (1.1) and (1.3). This time we take discontinuity at $d = 1/2$.

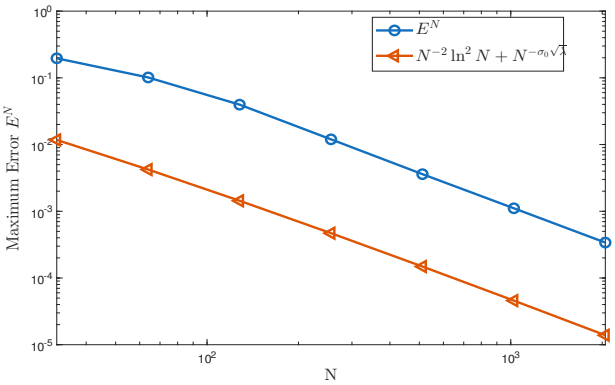
Figure 2a show the solution plot of the numerical solution to Example 5.2 for $\varepsilon = 10^{-10}$ and $N = 128$; note that for this example there are layers at $x = 0$, $x = 1$ and $x = 1/2$.

For both these examples, the exact solution is unavailable. The accuracy of the numerical solution is evaluated using the double mesh principle. To estimate the numerical error and compute the rate of convergence, we adopt the procedure described in Chapter 8 of [11]. Let D^N be a piecewise-uniform Shishkin mesh with N intervals, and define

Uncorrected Proof



(A) Solution of Example 5.2 with $\varepsilon = 10^{-10}$ and $N = 128$.



(B) log – log plot of Example 5.2.

FIGURE 2. Example 5.2.

TABLE 1. Errors E_ε^N in the computed solution to Example 5.1.

ε / N	32	64	128	256	512	1024	2048
10^{0}	8.073e−05	2.018e−05	5.045e−06	1.261e−06	3.153e−07	7.885e−08	1.970e−08
10^{-1}	2.721e−04	6.625e−05	1.628e−05	4.041e−06	1.008e−06	2.517e−07	6.291e−08
10^{-2}	1.230e−03	3.134e−04	7.853e−05	1.964e−05	4.909e−06	1.227e−06	3.067e−07
10^{-3}	1.249e−02	2.774e−03	6.762e−04	1.685e−04	4.209e−05	1.052e−05	2.630e−06
10^{-4}	3.828e−02	1.398e−02	4.176e−03	1.338e−03	4.213e−04	1.055e−04	2.635e−05
10^{-5}	3.828e−02	1.398e−02	4.176e−03	1.338e−03	4.213e−04	1.297e−04	3.923e−05
10^{-6}	3.828e−02	1.398e−02	4.176e−03	1.338e−03	4.213e−04	1.297e−04	3.923e−05
10^{-7}	3.828e−02	1.398e−02	4.176e−03	1.338e−03	4.213e−04	1.297e−04	3.923e−05
10^{-8}	3.828e−02	1.398e−02	4.176e−03	1.338e−03	4.213e−04	1.297e−04	3.923e−05
10^{-9}	3.828e−02	1.398e−02	4.176e−03	1.338e−03	4.213e−04	1.297e−04	3.923e−05
10^{-10}	3.828e−02	1.398e−02	4.176e−03	1.338e−03	4.213e−04	1.297e−04	3.923e−05
10^{-11}	3.828e−02	1.398e−02	4.176e−03	1.338e−03	4.213e−04	1.297e−04	3.923e−05
10^{-12}	3.828e−02	1.398e−02	4.176e−03	1.338e−03	4.213e−04	1.297e−04	3.923e−05
10^{-13}	3.828e−02	1.398e−02	4.176e−03	1.338e−03	4.213e−04	1.297e−04	3.923e−05
10^{-14}	3.828e−02	1.398e−02	4.176e−03	1.338e−03	4.213e−04	1.297e−04	3.923e−05
10^{-15}	3.828e−02	1.398e−02	4.176e−03	1.338e−03	4.213e−04	1.297e−04	3.923e−05
10^{-16}	3.828e−02	1.398e−02	4.176e−03	1.338e−03	4.213e−04	1.297e−04	3.923e−05
E^N	3.828e−02	1.398e−02	4.176e−03	1.338e−03	4.213e−04	1.297e−04	3.923e−05
p	1.972	2.242	2.034	2.008	2.004	2.000	

Uncorrected Proof

$\vec{Y}^N = (Y_1^N,\ Y_2^N)$ as the solution to (3.4) on this mesh. Similarly, consider D^{2N} with $2N$ intervals, which has the same transition point as D^N. The maximum pointwise error is computed for different values of ε and N as:

$$E_\varepsilon^N = \|\vec{Y}^N - \vec{Y}^{2N}\|_{D^N}.$$

The considered values of ε are $\varepsilon = 10^{-j}$, where $j = 0, -1, \ldots, -16$, while N takes values $N = 2^5, \ldots, 2^{11}$. The parameter-uniform error is defined as:

$$E^N = \max\left\{E_1^N,\ E_{10^{-1}}^N,\ \ldots,\ E_{10^{-16}}^N\right\}.$$

The rate of convergence is computed using the formula:

$$p = \frac{\ln E^N - \ln E^{2N}}{\ln(2\ln N) - \ln(\ln(2N))}.$$

Results for Example 5.1, solved for a range of values of N and ε, are shown in Table 1. Table 1 confirms that the convergence rate is second-order, as predicted in the theoretical analysis. This is a higher rate of convergence

TABLE 2. Comparison of error parameters using standard scheme and hybrid scheme for Example 5.1.

	Standard scheme		Hybrid scheme	
N	E^N	p	E^N	p
2^5	2.087e−02	1.352	3.828e−02	1.972
2^6	1.046e−02	1.907	1.398e−02	2.242
2^7	3.744e−03	1.895	4.176e−03	2.034
2^8	1.296e−03	1.971	1.338e−03	2.008
2^9	4.170e−04	1.992	4.213e−04	2.004
2^{10}	1.293e−04	1.996	1.297e−04	2.000
2^{11}	3.919e−05	—	3.923e−05	—

TABLE 3. Errors E_ε^N in the computed solution to Example 5.2.

ε / N	32	64	128	256	512	1024	2048
10^0	8.454e−04	2.121e−04	5.311e−05	1.329e−05	3.323e−06	8.310e−07	2.078e−07
10^{-1}	2.580e−03	6.467e−04	1.618e−04	4.045e−05	1.011e−05	2.528e−06	6.321e−07
10^{-2}	7.699e−03	1.981e−03	4.991e−04	1.250e−04	3.127e−05	7.820e−06	1.955e−06
10^{-3}	2.412e−02	7.907e−03	2.076e−03	5.346e−04	1.341e−04	3.356e−05	8.392e−06
10^{-4}	7.322e−02	2.833e−02	8.756e−03	2.991e−03	9.893e−04	2.503e−04	6.283e−05
10^{-5}	7.493e−02	2.885e−02	8.677e−03	2.778e−03	9.023e−04	2.798e−04	8.512e−05
10^{-6}	7.548e−02	2.901e−02	8.723e−03	2.791e−03	8.796e−04	2.721e−04	8.257e−05
10^{-7}	7.565e−02	2.906e−02	8.737e−03	2.796e−03	8.809e−04	2.703e−04	8.177e−05
10^{-8}	7.571e−02	2.908e−02	8.742e−03	2.797e−03	8.813e−04	2.704e−04	8.181e−05
10^{-9}	7.572e−02	2.909e−02	8.743e−03	2.798e−03	8.815e−04	2.704e−04	8.182e−05
10^{-10}	7.573e−02	2.909e−02	8.744e−03	2.798e−03	8.815e−04	2.704e−04	8.182e−05
10^{-11}	7.573e−02	2.909e−02	8.744e−03	2.798e−03	8.815e−04	2.704e−04	8.183e−05
10^{-12}	7.573e−02	2.909e−02	8.744e−03	2.798e−03	8.815e−04	2.704e−04	8.183e−05
10^{-13}	7.573e−02	2.909e−02	8.744e−03	2.798e−03	8.815e−04	2.704e−04	8.183e−05
10^{-14}	7.573e−02	2.909e−02	8.744e−03	2.798e−03	8.815e−04	2.704e−04	8.183e−05
10^{-15}	7.573e−02	2.909e−02	8.744e−03	2.798e−03	8.815e−04	2.704e−04	8.183e−05
10^{-16}	7.573e−02	2.909e−02	8.744e−03	2.798e−03	8.815e−04	2.704e−04	8.183e−05
E^N	7.573e−02	2.909e−02	8.756e−03	2.991e−03	9.893e−04	2.798e−04	8.512e−05
p	1.873	2.227	1.919	1.923	2.148	1.991	

Uncorrected Proof

than predicted in Theorem 4.1, and may be due to a simplification introduced by the problem featuring only constant coefficients. This is further verified graphically in Figure 1, which presents the numerical solution 1a and a log − log plot 1b for Example 5.1. It is evident from the table that the error remains robust and converges to zero as N increases.

Furthermore, the proposed hybrid difference scheme is compared with the standard difference scheme, which possesses an order of accuracy $O(N^{-2}\ln^2 N)$. The standard scheme employs a cubic spline approximation at the boundary points and the central difference scheme in the interior region. The comparison results for Example 5.1 are presented in Table 2, which clearly demonstrate that the proposed scheme outperforms the standard scheme.

Results for Example 5.2 are shown in Table 3. Again, we observe $\varepsilon-$uniform convergence, although in this case we note that the rate of convergence is almost second-order, which is in agreement with the theory. The log-log plot is given in Figure 2b. As done in Example 5.1, a comparison between the standard scheme and the proposed hybrid scheme is given in Table 4. From this table, again we confirm that the proposed hybrid scheme is superior to the standard scheme for problems of the form (1.1).

6. Conclusion

This paper introduces an efficient ε-uniform hybrid numerical scheme that combines the central difference scheme with the cubic spline technique to solve a set of singularly perturbed reaction-diffusion Robin problems (1.1) featuring a discontinuous point in each source term. The solution is computed on a piecewise−uniform mesh of Shishkin type, which is designed to capture both boundary and interior layers effectively. Theoretical analysis establishes that the

TABLE 4. Comparison of error parameters using standard scheme and hybrid scheme for Example 5.2.

	Standard scheme		Hybrid scheme	
N	E^N	p	E^N	p
2^5	3.799e−02	0.594	7.573e−02	1.873
2^6	2.804e−02	1.439	2.909e−02	2.227
2^7	1.291e−02	1.954	8.756e−03	1.919
2^8	4.325e−03	1.962	2.991e−03	1.923
2^9	1.399e−03	1.975	9.893e−04	2.148
2^{10}	4.383e−04	1.928	2.798e−04	1.991
2^{11}	1.384e−04	—	8.512e−05	—

scheme achieves almost second-order convergence, a result further validated by numerical problems in Section 5. These results confirm the efficiency of the proposed scheme. A natural progression of this work is to consider the more general case, where the singular perturbation parameters vary in each equation. This would enhance the applicability to a broader class of problems and we are working on it.

Data Availability

No data has been used.

Declaration of competing interest

The authors have no competing interests to declare that are relevant to the content of this article.

Uncorrected Proof

Funding sources

This research did not receive any specific grant from funding agencies in the public, commercial, or not-for-profit sectors.

References

[1] J. H. Ahlberg, E. N. Nilson, and J. L. Walsh, *The theory of splines and their applications*, Academic Press, 1967.
[2] A. R. Ansari and A. F. Hegarty, *Numerical solution of a convection diffusion problem with Robin boundary conditions*, J. Comput. Appl. Math., *156*(1) (2003), 221–238.
[3] A. R. Babu and N. Ramanujam, *A FEM for a system of singularly perturbed reaction-diffusion equations with discontinuous source term*, Int. J. Comput. Methods, *10*(5) (2013), 1350057.
[4] N. Barzehkar, A. Barati, and R. Jalilian, *Sinc approximation method for solving system of singularly perturbed parabolic convection-diffusion equations*, Appl. Numer. Math., *216* (2025), 127–139.
[5] P. M. Basha and V. Shanthi, *A uniformly convergent scheme for a system of two coupled singularly perturbed reaction–diffusion Robin type boundary value problems with discontinuous source term*, Am. J. Numer. Anal., *3*(2) (2015), 39–48.
[6] S. Chawla and S. C. S. Rao, *Numerical treatment for a coupled system of singularly perturbed reaction-diffusion equations with Robin boundary conditions and having boundary and interior layers*, Frontiers in Industrial and Applied Mathematics, Springer Proc. Math. Stat., *410* (2023), 629–645.
[7] C. Clavero, R. Shiromani, and V. Shanthi, *A numerical approach for a two-parameter singularly perturbed weakly-coupled system of 2-D elliptic convection-reaction-diffusion PDEs*, J. Comput. Appl. Math., *436* (2024), 115422.
[8] P. Das and S. Natesan, *A uniformly convergent hybrid scheme for singularly perturbed system of reaction-diffusion Robin type boundary-value problems*, J. Appl. Math. Comput., *41*(1–2) (2013), 447–471.

[9] P. Das, S. Rana, and J. Vigo-Aguiar, *Higher order accurate approximations on equidistributed meshes for boundary layer originated mixed type reaction diffusion systems with multiple scale nature*, Appl. Numer. Math., *148* (2020), 79–97.
[10] C. de Falco and E. O'Riordan, *Interior layers in a reaction-diffusion equation with a discontinuous diffusion coefficient*, Int. J. Numer. Anal. Model., *7*(3) (2010), 444–461.
[11] P. A. Farrell, A. F. Hegarty, J. J. H. Miller, E. O'Riordan, and G. I. Shishkin, *Robust computational techniques for boundary layers*, Applied Mathematics (Boca Raton), Chapman & Hall/CRC, 2000.
[12] F. W. Gelu and G. F. Duressa, *An accelerated numerical computation for singularly perturbed Robin-type parabolic problems with small parameters*, Res. Math., *11*(1) (2024), 2354536.
[13] F. W. Gelu and G. F. Duressa, *Efficient hybridized numerical scheme for singularly perturbed parabolic reaction–diffusion equations with Robin boundary conditions*, Partial Differ. Equ. Appl. Math., *10* (2024), 100662.
[14] A. Gupta, A. Kaushik, and M. Sharma, *A higher-order hybrid spline difference method on adaptive mesh for solving singularly perturbed parabolic reaction-diffusion problems with Robin-boundary conditions*, Numer. Methods Partial Differential Equations, *39*(2) (2023), 1220–1250.
[15] A. Jaiswal, S. Kumar, and H. Ramos, *Efficient uniformly convergent numerical methods for singularly perturbed parabolic reaction-diffusion systems with discontinuous source term*, J. Appl. Math. Comput., *71*(3) (2025), 3399–3427.
[16] A. Kaushik, A. Gupta, S. Jain, S. Toprakseven, and M. Sharma, *An adaptive mesh generation and higher-order difference approximation for the system of singularly perturbed reaction–diffusion problems*, Partial Differ. Equ. Appl. Math., *11* (2024), 100750.
[17] S. Kumar, R. Ishwariya, and P. Das, *Impact of mixed boundary conditions and nonsmooth data on layer-originated nonpremixed combustion problems: Higher-order convergence analysis*, Stud. Appl. Math., *153*(4) (2024), e12763.
[18] B. Lalrinhlua, A. M. Saeed, A. H. Ganie, R. Tiwari, S. Das, F. Mofarreh, and A. Singhal, *Study of vibrations in smart materials semiconductor under differential imperfect contact mechanism and nanoscale effect with electromechanical coupling effect*, Acta Mech., *236*(4) (2025), 2383–2403.
[19] N. Madden and M. Stynes, *A uniformly convergent numerical method for a coupled system of two singularly perturbed linear reaction-diffusion problems*, IMA J. Numer. Anal., *23*(4) (2003), 627–644.
[20] P. A. Markowich, *A singular perturbation analysis of the fundamental semiconductor device equations*, SIAM J. Appl. Math., *44*(5) (1984), 896–928.
[21] P. A. Markowich and C. A. Ringhofer, *A singularly perturbed boundary value problem modelling a semiconductor device*, SIAM J. Appl. Math., *44*(2) (1984), 231–256.
[22] S. Matthews, J. J. H. Miller, E. O'Riordan, and G. I. Shishkin, *A parameter-robust numerical method for a system of singularly perturbed ordinary differential equations*, Analytical and Numerical Methods for Convection-Dominated and Singularly Perturbed Problems (L. G. Vulkov, J. J. H. Miller, and G. I. Shishkin, eds.), Nova Science Publishers, 2000, 219–224.
[23] S. Matthews, E. O'Riordan, and G. I. Shishkin, *A numerical method for a system of singularly perturbed reaction-diffusion equations*, J. Comput. Appl. Math., *145*(1) (2002), 151–166.
[24] J. J. H. Miller, E. O'Riordan, and G. I. Shishkin, *Fitted numerical methods for singular perturbation problems*, revised ed., World Scientific Publishing Co. Pte. Ltd., 2012.
[25] M. Munawar, R. McNeil, T. A. E. Prasetya, R. Jani, D. McNeil, and N. Pongsiri, *Modelling land surface temperature variation in New Guinea Island from 2000 to 2019 using a cubic spline model*, Adv. Meteorol., *2024*(1) (2024), 5531961.
[26] S. Natesan and B. S. Deb, *A robust computational method for singularly perturbed coupled system of reaction-diffusion boundary-value problems*, Appl. Math. Comput., *188*(1) (2007), 353–364.
[27] S. C. S. Rao and S. Chawla, *Interior layers in coupled system of two singularly perturbed reaction-diffusion equations with discontinuous source term*, Numerical analysis and its applications, Lecture Notes in Comput. Sci., *8236* (2013), 445–453.
[28] W. Rodi, *Examples of turbulence-model applications*, Turbulence models and their applications, Vol. 2 (Bréau-sans-Nappe, 1982), Collect. Dir. Études Rech. Élec. France, vol. 56, Eyrolles, Paris, 1984, 295–401, 415–419.

Uncorrected Proof

[29] H. G. Roos, M. Stynes, and L. Tobiska, *Robust numerical methods for singularly perturbed differential equations*, Springer-Verlag, 2008.
[30] S. Saini, P. Das, and S. Kumar, *Parameter uniform higher order numerical treatment for singularly perturbed Robin type parabolic reaction diffusion multiple scale problems with large delay in time*, Appl. Numer. Math., *196*(1) (2024), 1–21.
[31] R. Shiromani, N. Madden, and V. Shanthi, *A finite difference scheme for two-dimensional singularly perturbed convection-diffusion problem with discontinuous source term*, arXiv preprint arXiv:2401.02331, 2024.
[32] R. Soundararajan and V. Subburayan, *Efficient finite element method for 2D singularly perturbed parabolic convection diffusion problems with discontinuous source term*, Comput. Appl. Math., *43*(6) (2024), 384.
[33] K. R. Sreenivasan and J. Schumacher, *What is the turbulence problem, and when may we regard it as solved?*, Annu. Rev. Condens. Matter Phys., *16*(1) (2025), 121–143.
[34] G. P. Thomas, *Towards an improved turbulence model for wave-current interactions*, Tech. report, The Kinematics and Dynamics of Wave-Current Interactions, EU MAST-III Project, 1998.
[35] J. Turner and S. LaBrake, *Elementary computational fluid dynamics using finite-difference methods*, Honors thesis, Union College, 2018.
[36] S. Veerasamy and N. Srinivassan, *Solution of singularly perturbed system of 2D parabolic convection diffusion differential-difference equations using alternating direction method*, Indian J. Pure Appl. Math., (2024), 1–18.
[37] N. S. Yadav and K. Mukherjee, *Parameter-robust higher-order time-accurate computational method for singularly perturbed time-dependent semilinear convection-diffusion PDEs with discontinuous data*, Math. Methods Appl. Sci., *47*(11) (2024), 9249–9274.

Uncorrected Proof